

Optimization of Sound Transmission Loss of a Composite Rectangular Plate with Infinite Baffle

A. Nouri^{1*} and S. Astaraki²

1, 2. Shahid Sattary University of Science and Technology

*Postal Code: 64891-14666, Tehran, IRAN

*anouri@ssau.ac.ir

In this paper, optimization of the sound transmission loss of finite rectangular anisotropic laminated composite plate with simply supported boundary conditions has been developed to maximize transmission loss. Appropriate constraints were imposed to prevent the occurrence of softening effect due to optimization. For this purpose, optimization process was incorporated into comprehensive finite element software. The transmission loss (TL) obtained from the numerical solution was compared with those of other authors indicated good agreement. The discrete frequencies have been chosen based upon the sound transmission class with A-weighting constant. Several traditional composite materials have been studied and the results have shown that in the mass control region, the optimization of stacking sequence and optimal thickness has not been an effective contribution to improve the transmission loss. The results also show that, the lamina thickness optimization has an important effect on improving the transmission loss, but the advantage of low weight composite material is compromised by optimization.

Keywords: Optimization, Transmission Loss, Baffle, Composite Panel

Introduction

The interaction between composite panel vibrations and the surrounding medium is an important subject that arises in many practical applications. These panels are intended to not only meet the structural requirements, but also to radiate minimum noise and provide acoustic insulation from the surrounding environment [1]. Therefore, analysis of the vibro-acoustic behavior of panels is an integral part of the design of structures [2]. Consequently, some analytical models have been developed to predict the TL characteristics of composite walls. These analytical models were generally divided as either high-frequency-noise or low-frequency-noise models. In high-frequency noise, the dimensions of the walls are very large relative to the sound

wavelengths, so, the wall can be modeled as infinite. The analytical models based on infinite-panel theory have been extensively developed by Smith [3], White [4], Koval [5], Blaise [6], Lee and Kim [7] and dealt with such features as isotropic, orthotropic, and anisotropic shells and plates. In low-frequency noise, the dimensions of the wall are comparable with the large sound wavelengths. In order to calculate the TL of these panels, the analytical model must take into account the boundary conditions of the wall. Thus, a finite panel transmission loss theory is needed. Such a theory has been developed by Roussos [8] and is currently being implemented. In this approach, the wall is modeled as a rectangular plate with the simply supported boundary conditions in an infinite baffle. Hence, optimization studies of TL characteristics of composite materials with respect to their material and geometry properties have been an important topic of research for a few decades. Most of these

1. Assistant Professor (Corresponding Author)
2. Assistant Professor

studies have been related to high frequency noise model [9-12]. The sound transmission loss through sandwich panels has been studied by Dym and lang [13]. They used isotropic panels with Young's modulus, mass density and thicknesses of the skins and the core as design variables. Wang et al. [10] used a generic algorithm to optimize a sandwich panel with balanced acoustic and mechanical properties at a minimal weight. Tsai [11] used conjugate gradient optimization method to estimate and optimize transmission loss of material properties of the composite plate. The vibration and acoustic behavior of Functionally Graded Materials (FGM) has become a subject of interest in the recent years. Nouri et al. [12] optimized sound transmission loss of functionally graded materials cylindrical shell. Chandra et al. [1] studied vibro-acoustic and sound transmission loss characteristics of FGM plates using a simple first-order shear deformation theory. Chakraborty and Gopalakrishnan [13] studied wave propagation in functionally graded materials using spectral layer elements. Moreover, some researchers have investigated impedance models of acoustic structures. This approach assumes an acoustic structure of infinite size; it expresses the transmission of pressure and vibrations via transfer matrices. Geebelen et al. [14] considered layers of poroelastic materials in the acoustic structure. Talebitooti et al. used the three-dimensional elasticity theory to calculate the sound transmission loss of the multilayered cylindrical shell with porous core and air-gap [15]. Dijkmans et al. [16] compared the results of the transfer matrix method with those of a wave-based model for sound transmission through finite light weight multilayered structures assembled with thin air layers. Literature shows that no work has been done to study the optimization of sound transmission loss of finite rectangular anisotropic laminated composite plate.

Talebitooti and Zarastvand analyzed the wave propagation on infinite doubly curved laminated composite shell sandwiching a porous material [17]. The acoustic behavior of laminated composite infinitely long doubly curved shallow shells subject to a radiating oblique plane sound wave is also studied by these researchers [18]. The objective of this study is to obtain stacking sequence and plies thickness of layers for achieving the maximum TL for anisotropic

composite rectangular finite plate with infinite baffle. The present work has developed Roussos's model [8] to optimize the transmission characteristics of an anisotropic plate. The solution is expanded into infinite series form using the modal series expansion. Consequently, convergence checking is performed to truncate these infinite series. Optimizations performed at discrete frequencies chosen in the bound 1-4 kHz are identical to those used to define a single insulation measure in an ASTM standard [9]. The genetic algorithm is utilized as the optimization technique with plies angle, lamina thickness, material layers as design parameters and buckling as a constrain [20]. However, analytical optimization process is restricted to simple models, consequently, it must be conjugated with comprehensive structural analysis software. Therefore, it is very important to model a proper mechanical part of problem in finite element package. This paper also represents the basis at which such combination can be done. In this approach, the buckling analysis and natural frequencies of anisotropic material has been determined using finite element model in the optimization process. So, they are directly obtained without any approximation [21]. As the densities of composite materials are closer to each other, the result shows that in the mass control region, optimization of plies orientation and plies thickness has no significant effect on the TL, so, to improve the TL of composite material, it is better to use high stiffness materials.

Analytical Model Description

The analytical model developed by Roussos (1985) is based on modal summation method that allows for the efficient calculation of the transmission characteristics of a rectangular simply supported plate in an infinite rigid baffle. In this study, Roussos' model has been developed for anisotropic panel. According to [22], the thin plate theory for anisotropic plate, the equation of motion, must be rewritten to account for stiffness terms as follows:

$$\begin{aligned}
 & D_{11} \frac{\partial^4 w}{\partial \xi^4} + 4D_{16} \frac{\partial^4 w}{\partial \xi^3 \partial \eta} + 2(D_{12} + 2D_{66}) \frac{\partial^4 w}{\partial \xi^2 \partial \eta^2} \\
 & + 4D_{26} \frac{\partial^4 w}{\partial \xi \partial \eta^3} + D_{22} \frac{\partial^4 w}{\partial \eta^4} + C_D \frac{\partial w}{\partial t} + m_p \frac{\partial^2 w}{\partial t^2} \quad (1) \\
 & = p_i(\xi, \eta, t) + p_r(\xi, \eta, t) - p_l(\xi, \eta, t)
 \end{aligned}$$

where p_i , p_r and p_t are the incident, reflected and transmitted pressures, respectively (Fig. 1).

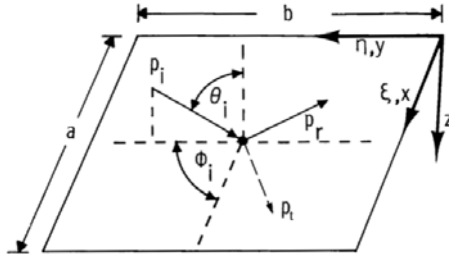


Figure 1. Geometry of plane wave incident on a panel [8]

These three pressures can be rewritten as the sum of the blocked pressure (the pressures on the incident side) and the radiated pressure (the pressure due to plate vibrating). Because the radiated pressure is an unknown function of the plate displacement, Roussos assumed that the radiated pressure is negligible compared with the blocked pressure. This assumption allows an accurate solution to be obtained over a large frequency range and gives invalid answers only for frequencies near the fundamental resonant frequency. Therefore, the block pressure is only the forcing function in Eq. (1)

$$D_{11} \frac{\partial^4 w}{\partial \xi^4} + 4D_{16} \frac{\partial^4 w}{\partial \xi^3 \partial \eta} + 2(D_{12} + 2D_{66}) \frac{\partial^4 w}{\partial \xi^2 \partial \eta^2} + 4D_{26} \frac{\partial^4 w}{\partial \xi \partial \eta^3} + D_{22} \frac{\partial^4 w}{\partial \eta^4} + C_D \frac{\partial w}{\partial t} + m_p \frac{\partial^2 w}{\partial t^2} = p_b(\xi, \eta, t) \quad (2)$$

Where the blocked pressure is twice the incident pressure [23]. The incident pressure is assumed to be an obliquely incident plane wave given by:

$$p_i(\xi, \eta, t) = P_i \exp[i(\omega t - k\xi \sin \theta_i \cos \phi_i - k\eta \sin \theta_i \sin \phi_i)] \quad (3)$$

Where k is the wave number and ω is the angular frequency. Since the forcing pressure is harmonic, the steady-state plate displacement will be harmonic too;

$$w(\xi, \eta, t) = W(\xi, \eta) \exp(i\omega t) \quad (4)$$

Substituting equations (3) and (4) into (2) and dividing by $\exp(i\omega t)$ gives

$$D_{11} \frac{\partial^4 W}{\partial \xi^4} + 4D_{16} \frac{\partial^4 W}{\partial \xi^3 \partial \eta} + 2(D_{12} + 2D_{66}) \frac{\partial^4 W}{\partial \xi^2 \partial \eta^2} + 4D_{26} \frac{\partial^4 W}{\partial \xi \partial \eta^3} + D_{22} \frac{\partial^4 W}{\partial \eta^4} + iC_D \omega \frac{\partial W}{\partial t} + m_p \omega^2 \frac{\partial^2 W}{\partial t^2} = 2P_i \exp[ik \sin \theta_i (\xi \cos \phi_i - \eta \sin \phi_i)] \quad (5)$$

For the simply supported panel, the displacement of the panel can be written in terms of an infinite series of its vibration modes multiplied by the modal participation factor (W_{mn})

$$W(\xi, \eta) = \sum_{m=1}^{\infty} \sum_{n=1}^{\infty} W_{mn} \sin\left(\frac{m\pi\xi}{a}\right) \sin\left(\frac{n\pi\eta}{b}\right) \quad (6)$$

The forcing pressure can also be represented by an infinite series of the eigen functions as follow:

$$2P_i \exp[ik \sin \theta_i (\xi \cos \phi_i - \eta \sin \phi_i)] = \sum_{m=1}^{\infty} \sum_{n=1}^{\infty} p_{mn} \sin\left(\frac{m\pi\xi}{a}\right) \sin\left(\frac{n\pi\eta}{b}\right) \quad (7)$$

Where p_{mn} , the generalized forcing pressure, is given by

$$p_{mn} = \frac{8P_i}{ab} \int_{\xi=0}^a \int_{\eta=0}^b \exp[ik \sin \theta_i (\xi \cos \phi_i - \eta \sin \phi_i)] \sin\left(\frac{m\pi\xi}{a}\right) \sin\left(\frac{n\pi\eta}{b}\right) d\eta d\xi \quad (8)$$

The closed form integration of equation (8) can be done as:

$$\bar{I}_m = \begin{cases} \frac{-i \operatorname{sgn}(\sin \theta_i \cos \phi_i)}{2} & , ((m\pi)^2 = [\sin \theta_i \cos \phi_i (\omega a/c)]^2) \\ \frac{m\pi \{1 - (-1)^m \exp[-i \sin \theta_i \cos \phi_i (\omega a/c)]\}}{(m\pi)^2 - [\sin \theta_i \cos \phi_i (\omega a/c)]^2} & , ((m\pi)^2 \neq [\sin \theta_i \cos \phi_i (\omega a/c)]^2) \end{cases} \quad (9)$$

$$\bar{I}_n = \begin{cases} \frac{-i \operatorname{sgn}(\sin \theta_i \cos \phi_i)}{2} & , ((n\pi)^2 = [\sin \theta_i \cos \phi_i (\omega b/c)]^2) \\ \frac{n\pi \{1 - (-1)^n \exp[-i \sin \theta_i \cos \phi_i (\omega b/c)]\}}{(n\pi)^2 - [\sin \theta_i \cos \phi_i (\omega b/c)]^2} & , ((n\pi)^2 \neq [\sin \theta_i \cos \phi_i (\omega b/c)]^2) \end{cases}$$

The modal participation factor can be obtained by substituting equations (7) and (8) into equation (5)

$$W_{mn} = \frac{P_{mn}}{m_p \left[\omega_{mn}^2 - \omega^2 + \left(\frac{iC_D \omega}{m_p} \right) \right]} \quad (10)$$

Where ω_{mn} is natural frequencies of the simply supported anisotropic plate. Roussos calculated transmission loss of composite materials based on Bert (1977) approximate equation for the modal resonant frequencies. In this paper, natural frequencies are calculated by finite element analysis and the results are conjugated with analytical solution. Thus, the solution for plate vibration is performed. Transmitted pressure at a point distant from the panel due to the vibration of the plate is calculated using the Rayleigh integral and can be written as [24].

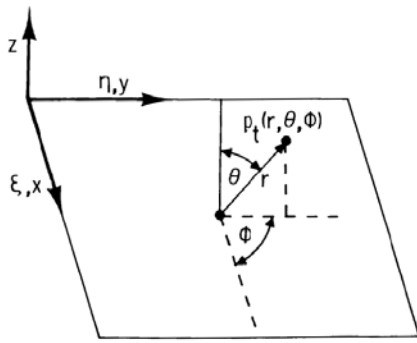


Figure 2. Geometry of radiating side of plate [8]

$$p_t(r, \theta, \phi) = \frac{-\alpha \rho a b}{2\pi r} \exp\left\{i\omega t - \frac{r}{c} - \frac{\sin\theta}{2c}(a\cos\phi + b\sin\phi)\right\} \sum_{m=1}^{\infty} \sum_{n=1}^{\infty} W_{mn} I_m I_n$$

$$I_m = \begin{cases} \frac{i}{2} \operatorname{sgn}(\sin\theta \cos\phi) & , ((m\pi)^2 = [\sin\theta \cos\phi(\omega a/c)]^2) \\ \frac{m\pi \{1 - (-1)^m \exp[-i \sin\theta \cos\phi(\omega a/c)]\}}{(m\pi)^2 - [\sin\theta \cos\phi(\omega a/c)]^2} & , ((m\pi)^2 \neq [\sin\theta \cos\phi(\omega a/c)]^2) \end{cases} \quad (11)$$

$$I_n = \begin{cases} \frac{-i}{2} \operatorname{sgn}(\sin\theta \cos\phi) & , ((n\pi)^2 = [\sin\theta \cos\phi(\omega b/c)]^2) \\ \frac{n\pi \{1 - (-1)^n \exp[-i \sin\theta \cos\phi(\omega b/c)]\}}{(n\pi)^2 - [\sin\theta \cos\phi(\omega b/c)]^2} & , ((n\pi)^2 \neq [\sin\theta \cos\phi(\omega b/c)]^2) \end{cases}$$

The transmitted intensity is calculated as:

$$I^t = \left| \sum_{m=1}^{\infty} \sum_{n=1}^{\infty} p_t \right|^2 / (2\rho c) \quad (12)$$

The transmitted acoustic power (Π_t), can now be calculated by integrating the transmitted intensity over a far-field hemisphere such that:

$$\Pi_t = \int_{\phi=0}^{2\pi} \int_{\theta=0}^{\pi/2} I^t r^2 \sin\theta \, d\theta \, d\phi \quad (13)$$

This equation must be integrated numerically. Finally, transmission loss is calculated as following:

$$TL = 10 \log \frac{\Pi_i}{\Pi_t} \quad (14)$$

Where Π_i is the incident acoustic power that is simply given as:

$$\Pi_i = \frac{P_i^2 ab \cos\theta_i}{2\rho c} \quad (15)$$

The method of calculating the transmission loss of the panel can be summarized as:

1. Calculating the generalized forcing pressure using Eq. (9)
2. Calculating the incident acoustic power by means of Eq. (15)
3. Applying the generalized forcing pressure to the panel and calculating the vibration response using Eq. (10) and finite element model.
4. Calculating the pressure, intensity, and radiated power using equations (12) and (13)

5. Calculating the transmission loss of the panel by means of Eq. (14)

In order to verify the validity of the present study, the result for isotropic plate has been compared with Roussos' study [8]. The oblique-incidence transmission loss of an aluminum plate with 380×150 and 0.81 mm thickness has been calculated for an incident wave at $\theta_i = 60^\circ$ and $\phi_i = 0$. The results are shown in Fig. 3 along with a transmission loss calculation based on Roussos model. The two curves agree well in both mass and stiffness controlled regions.

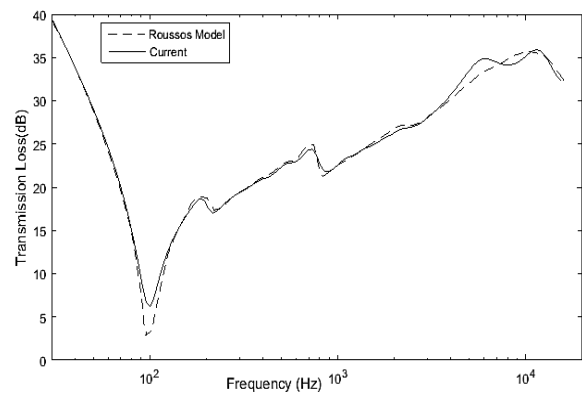


Figure 3. Comparison of current study with Roussos model

As one can see in Eq. (10), the solutions are obtained in series form. Therefore, one has to ensure that enough numbers of modes are included in the analysis to make the solution converge. When insufficient number of modes is used in the calculation, the resulting TL becomes overestimated. Therefore, we construct an iterative procedure in each frequency. When the TLs calculated at two successive calculations are within a pre-set error bound, the solution is considered to have converged. Changes in the calculated TL as the number of modes increases are shown in Fig. 4 at 1000 and 10000 frequencies, which indicate that by increasing the frequency, the number of modes for convergence is increased.

Figure 5 shows the effects of materials on TLS. The Materials chosen for the comparison are Graphite epoxy, Fiberglass epoxy, Kevlar epoxy, Fiber carbon and Aluminum as shown in Table 1. The plies were arranged in a $[0^\circ, 90^\circ, 0^\circ, 90^\circ]_s$. The dimensions of the panel are assumed to be 360×200 mm with simply supported boundary condition and the thickness of each ply is 0.125 mm.

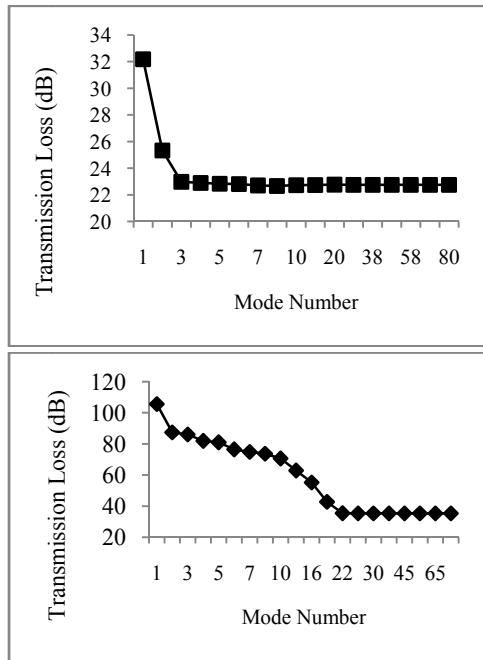


Figure 4. Mode convergence diagram; Left (f=1000 Hz), Right (f=10000 Hz)

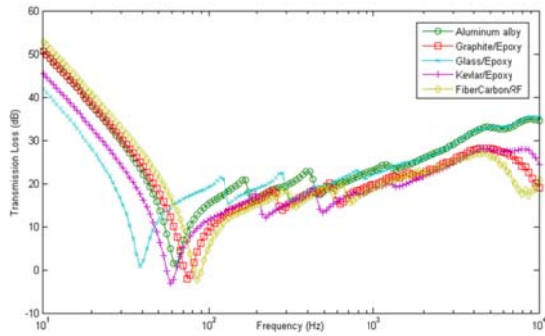


Figure 5. TL behavior of cross ply composite material

Table 1. Mechanical properties of rectangular panel [22]

Material	E_{11} (GPa)	E_{12} (GPa)	G_{12} (GPa)	ν_{12}	ρ (kg/m ³)
Aluminum	70	70	26.9	0.33	2760
Graphite/Epoxy	137	10	5	0.3	1550
Fiberglass/Epoxy	39	9	2	0.34	2190
Kevlar/Epoxy	76	6	2	0.3	1360
FiberCarbon/RF	206	5.17	2.58	0.25	1523

The figure indicates that aluminum is most effective in the high frequency range and fiber carbon is most effective in the low frequency range. This is as expected because the density of aluminum and the stiffness of the fiber carbon are higher than the other materials which make them most effective in the mass and stiffness controlled regions, respectively. The figure also shows that fiberglass, which has the lowest stiffness has the minimum effect on TL in the low frequency range, which is expected, because the low frequency range is controlled by stiffness.

Fig. 6 shows the angle ply orientation on the TL. The plies were arranged in a $[45^\circ, -45^\circ, 45^\circ, -45^\circ]_S$. The angle orientation of the plies is seen to have a significant effect on the fundamental frequency of the plate. Because the panel behaved in a mass law manner in the mass controlled region, the stiffness and the ply orientations of the panel have no effect on TL in this region.

Although the ply angle layout has no effect on TL in the mass controlled region, it may affect the value of the critical frequency and the TL in the stiffness control region. The ply angles and the bending stiffness are given in Table 2.

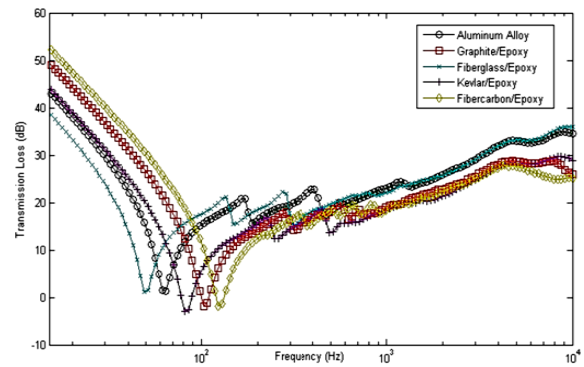


Figure 6. TL behavior of angle ply composite materials

Table 2. The Rigidity values of angle ply and cross ply panel

Material	Orientation	D11	D12	D16	D22	D26	D66	Freq. (Hz)	Buckling load (N)
Graphite	[0 90 0 90]s	8.16	0.25	0	4.17	0	0.42	74.77	3484
	[45 -45 45 -45]s	3.62	2.79	0.99	3.62	0.99	2.95	103.69	5068
Kevlar	[0 90 0 90]s	4.55	0.17	0	2.34	0	0.17	59.21	2087
	[45 -45 45 -45]s	1.97	1.64	0.55	1.97	0.55	1.64	82.55	2731
Fiberglass	[0 90 0 90]s	2.52	0.22	0	1.56	0	0.17	38.94	1355
	[45 -45 45 -45]s	1.30	0.97	0.24	1.30	0.24	0.91	49.61	1769
Fiber Carbon	[0 90 0 90]s	11.95	0.11	0	5.67	0	0.21	85.3	5031
	[45 -45 45 -45]s	4.675	4.25	1.57	4.67	1.57	4.35	124.97	6389

The Optimization Problem

To optimally design a structure with a maximum TL, we have to deal with a multivariable optimization problem. The optimization problem can be stated as:

$$\min f(X) = -STL(X), X = [x_1, x_2, \dots, x_n], X \in R^n \quad (16)$$

Since the weight and the stiffness of the composite structures are the important concern in most applications, they must be considered in the optimization process. So, to prevent the softening effect related to the base line plate and preserve the low weight advantage of composite material, we introduce additional constrains as follows:

$$\min f(X) = -STL(X), X = [x_1, x_2, \dots, x_n], X \in R^n \quad (17)$$

$$s.t. \quad c_i(X) = \begin{cases} W(X) - W_0 \leq 0 \\ F_0 - F(X) \leq 0 \end{cases} \quad (18)$$

Where $f(x)$ is the objective function to be minimized with respect to the vector x of the design variables, and the $W(X)$ and $F(X)$ are weight and critical buckling load as two inequality constraints, respectively. Note that the critical buckling load of a structure is a common measure of the stiffness of the structure. W_0 and F_0 are two constants and refer to the mass per unit width and critical buckling load. In this study, the first buckling mode of the FiberCarbon/ Epoxy with the same plate dimensions is considered as a reference. In the present paper, we study the optimization problem of a symmetric 8 ply composite laminate plate with respect to the geometric and material properties. The design variables for this problem are fiber angles, fiber thicknesses and material plies.

$$X = [\theta_i, h_i, m_i], i = 1, \dots, 4 \quad X_{lb} \leq X \leq X_{ub} \quad (19)$$

X_{lb} and X_{ub} are vectors, which define the lower and upper bounds of the design variables. There are many optimization techniques for different problems. In this study, the Augmented Lagrangian Genetic Algorithm has been used as optimization method [25]. In this approach, the constrained minimization problem can be converted into unconstrained one (subproblem) by adding the Lagrangian parameter which accounts for violation of the constraint. A sequence of such optimization problems are approximately minimized using the genetic algorithm such that the constraints and bounds are satisfied. A subproblem formulation is defined as.

$$\Theta(X, \lambda, s) = f(X) - \sum_{i=1}^2 \lambda_i s_i \log(s_i - c_i(X)) \quad (20)$$

Where the components λ_i are nonnegative and are known as Lagrange multiplier estimates, the elements s_i are nonnegative shifts. The algorithm begins with using an initial value for the penalty parameter. The genetic algorithm minimizes a sequence of subproblems, each of which is an approximation of the original problem. Each subproblem has a fixed value of λ and s . When the subproblem is minimized to a required accuracy and satisfies feasibility conditions, the Lagrangian estimates are updated. Otherwise, the penalty parameter is increased. These steps are repeated until the stopping criteria are met. Each subproblem solution represents one generation. As anisotropic materials do not have analytical solution for buckling analysis; stability analysis is performed using ANSYS APDL. As shown in Fig. 7, optimization processes were incorporated into comprehensive finite element software.

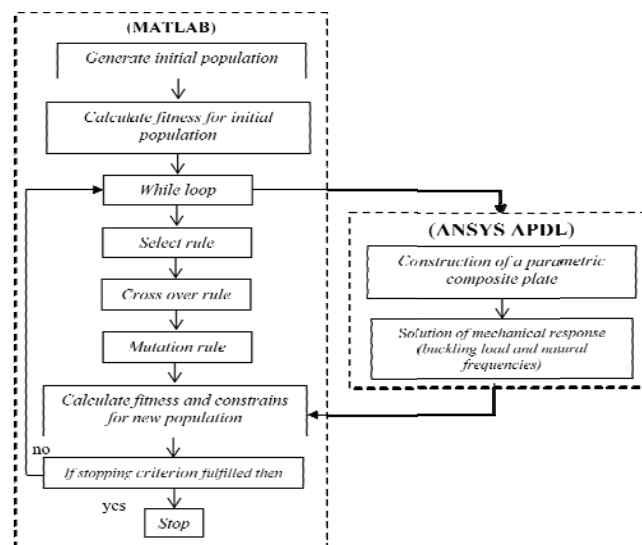


Figure 7. Optimization flowchart using MATLAB and ANSYS APDL

Frequency Range

It should be emphasized here that the TL is a strong function of frequency. Thus, to measure the TL various methods are used, each one incorporating a different set of standardized frequencies. For practical purposes, hearing encompasses a range of frequencies from about 16 Hz to somewhat less than 20000 Hz. However, low frequencies do not affect human ears very strongly, while those from 500-5000 Hz (where the ear is most sensitive) are very important. For the Sound Transmission Class (STC), the single-number rating system compares the TL of a test specimen with a standard contour. This study used the frequency range 1- 4 KHz. However, instead of the 21 frequencies (150 Hz steps) used then, only the seven standardized frequencies from the STC rating in the 1000 to 4000 Hz range would be incorporated. Namely, the following frequencies are considered: 1000, 1250, 1600, 2000, 2500, 3150, and 4000 Hz. The smaller number of frequencies does not lessen the accuracy in the calculations of TL because a sophisticated integration algorithm was used to find the field-incidence average TL. Also, the use of these frequencies parallels the portion of the spectrum emphasized in the recent ASTM standard E597-81[26] on isolation between neighboring rooms.

The lower limit of the range (1000Hz) was chosen in part because of the experimental results cited by [27]. In this case, the objective function is modified as.

$$\min f(X) = -10 \log_{10} |\tau_{avg}(X)| \tag{21}$$

$$\tau_{avg}(X) = \sum_{i=0}^{N_f} \bar{\beta}_i \frac{\Pi_i}{\Pi_t} \tag{22}$$

Where $\bar{\beta}_i$ represents weighting constants and N_f is the number of frequencies. $\bar{\beta}_i$ is normalized so that the sum of all the coefficients is unity. The weighting constants $\bar{\beta}_i$ are commonly chosen to correspond to an A-weighting. It should be mentioned here that with A-weighting, the sound-level meter is relatively less sensitive to sounds of frequencies below 1000 and above 4000 Hz. The weighting and discrete frequencies that were

chosen in the bound 1-4 kHz are identical to those used to define a single insulation measure in an ASTM standard [19,27], The normalized weights $\bar{\beta}_i$ are given in Table 3.

Table 3. Normalized weights using the A-weighting

Frequency (Hz)	A-weighting dB (A)	Multiplier $10^{dB(A)/10}$	β_i
1000	0	1	0.1156
1250	0.6	1.148	0.1327
1600	1	1.259	0.1455
2000	1.2	1.318	0.1524
2500	1.3	1.349	0.1559
3150	1.2	1.318	0.1524
4000	1	1.259	0.1455

Result and Discussion

Numerical simulations have been carried out to study the optimization problem of a rectangular composite plate. Based on the result in Figs 3 and 4, Graphite/Epoxy and Fiber carbon/RF are recommended as composite materials for maximum TL. As a demonstration of such applications, design parameter studies were conducted. The basic dimensions and simulation conditions used in the study are listed in Table 4.

Two different types of optimization are used in this paper. The first one is used to maximize the TL of a laminated composite plate by adjusting the stacking sequence of layers made of single material, while the second one is used for multiple materials.

Single Material

The objective of this case is to maximize the TL by varying the ply orientations and ply thickness for a given material and number of layers. At the first stage, a symmetric 8-ply constant thickness laminate layer is optimized with plies orientation as the design variables which is described by the vector.

$$x_i = [\theta_1, \theta_2, \theta_3, \theta_4]_s \quad -90 \leq \theta_i \leq 90 \tag{23}$$

As mentioned earlier, to prevent softening of plate due to parameters optimization, angle-ply buckling load is considered as a constraint. Table 5 shows the ply orientation for the optimized laminated plate with critical buckling load and fundamental frequency.

Table 4. Material and Environmental Properties

Material			Plate Materials						Ambient
			Graphite / Epoxy			Fiber Carbon / RF			Air
ρ (kg/m ³)			1550			1523			2.9
E_{11} (GPa)	E_{12} (GPa)	G_{12} (GPa)	137	10	5	206	5.17	2.58	-
ν			0.3			0.25			-
Sound Speed (m/s)			-			-			340
Incident Angle (deg.)			60						
Plate dim. (m)			0.36 × 0.2						
plate Thickness (mm)			1 or variable						

Table 5. Optimized ply orientation for composite plate with constant thickness plies

Material	Optimized ply orientation	buckling load (N)	Freq. (Hz)	Surface density Kg/m ²
Graphite /Epoxy	[55 -52 62 8]s	5101	100.87	1.59
Fiber carbon/RF	[60 -56 62 18]s	6307	122.86	1.52

The TL curve for the optimized ply orientation is shown in Figs 8 and 9 for Graphite/Epoxy and Fiber carbon/RF, respectively.

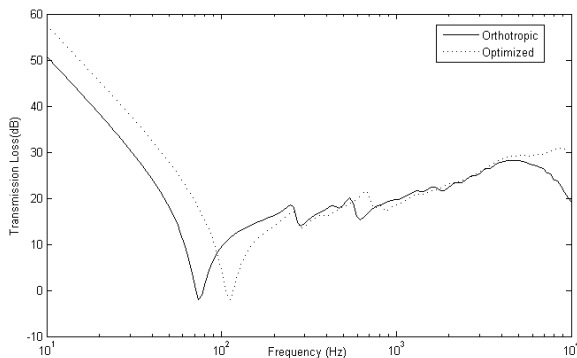


Figure 8. Optimized transmission loss for Graphite/Epoxy.

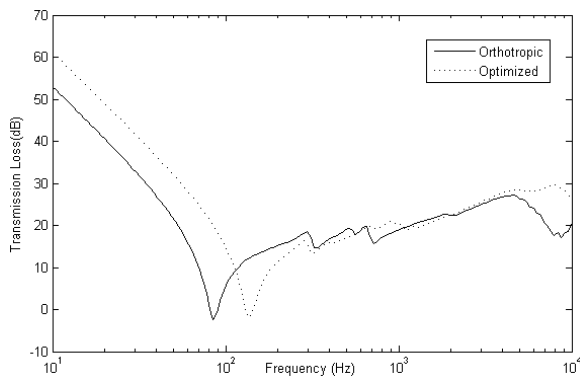


Figure 9. Optimized transmission loss for Fiber carbon/RF.

The results show that, the optimized orientation has 25% and 30% increases in fundamental frequency of Graphite/Epoxy and Fiber carbon/RF, respectively and thus, has a much higher transmission loss in the stiffness-controlled region. In the mass control region, two curves merge together since both panels have the same weight per unit area. Lamina thickness variation is another approach for better TL. In addition to lies orientation, the thicknesses of the layers are considered as design variables, too. However, it will affect the advantage of low weight composite material. So, a constraint of total weight of the structure is also imposed as:

$$c_1 = \sum_{i=1}^8 h_i \rho_i - m_0 \leq 0 \tag{24}$$

Where $m_0 = 1.5 \text{ kg/m}^2$ is the mass per unit area. The design variables for this problem are chosen as:

$$x_i = [\theta_1, \theta_2, \theta_3, \theta_4, h_1, h_2, h_3, h_4]_s \quad -90 \leq \theta_i \leq 90, \quad 0.1^{mm} \leq h_i \leq 0.2^{mm} \tag{25}$$

The optimization results for this case are shown in Table 6.

Table 6. Optimized ply orientation for composite plate

Material	Optimized ply Orientation (deg.)	Optimized ply Thickness (mm)	buckling show load (N)	Freq. (Hz)	Surface density Kg/m ²
Graphite /Epoxy	[6059-6753]s	[0.124 0.132 0.138 0.172]s	5117.9	114.32	1.796
Fiber carbon/RF	[61 -83 63 -33]s	[0.170 0.111 0.131 0.179]s	6322.8	143.76	1.796

Figs 10 and 11 presents the TL of optimized plate. The result clearly reveals that the TL increases with increasing plate thickness. The increase in TL of the Graphite/Epoxy and Fiber carbon/RF with respect to orthotropic plate is about more than 6 dB and 11dB in the stiffness control region respectively.

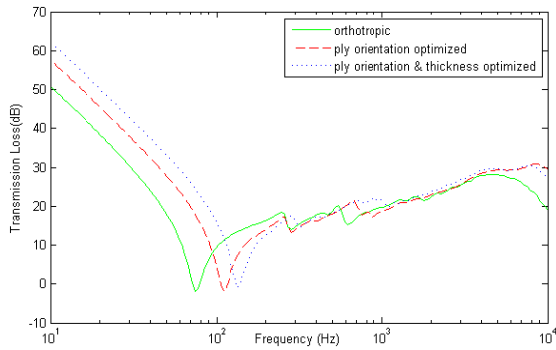


Figure 10. Optimized transmission loss for Graphite/Epoxy

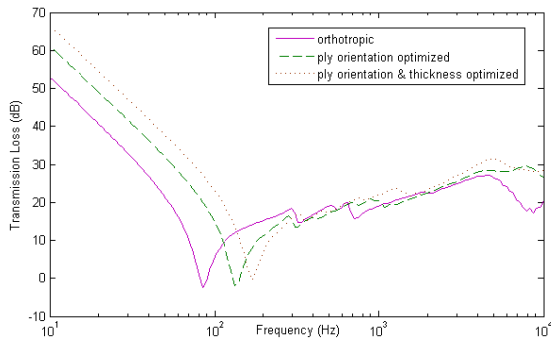


Figure 11. Optimized transmission loss for Fiber carbon/RF.

Multi Materials

In this section, the ability of the proposed optimization method to obtain the maximum transmission loss of a multiple composite plate is evaluated. The purpose of the designed optimization is to find another feasible and efficient composite multi materials plate to improve TL. The estimated composite materials of plate should have the stability requirement with low weight.

The design variables for this problem are considered as:

$$x_i = [\theta_1, \theta_2, \theta_3, \theta_4, h_1, h_2, h_3, h_4, n_1, n_2, n_3, n_4]_s \quad (26)$$

where n represents the selected material as in Table 2. The optimization results for this case are tabulated in Table 7. The results show the material stiffness has a significant role in TL optimization process.

Fig. 12 illustrates the TL of the optimized multimaterial plate. As shown, these results have only small differences with respect to Fiber carbon material optimization.

Table 7. Multi-material Optimization

Optimized orientation	Optimized thickness (mm)	Fun. Freq. (Hz)	Surface density Kg/m ²	Optimized layers material density			
				1 st	2 nd	3 th	4 th
[63 68 -59 39]s	[0.133 0.164 0.175 0.119]s	143.1	1.802	1520	1520	1520	1550

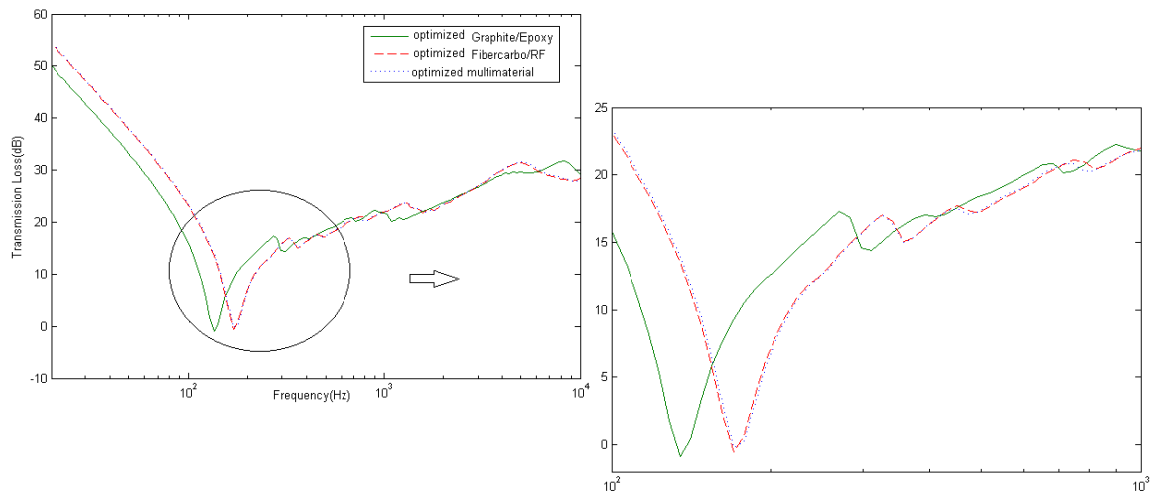


Figure 12. Optimized transmission loss of multi-material

Conclusion

The optimization study of sound transmission loss across a finite composite rectangular plate has been presented in this paper. A Roussos analytical model of TL with infinite baffle has been used for the optimization. To make sure enough number of modes have been included in the analysis, the convergence checking has been performed. The genetic algorithm has been used as the optimization method. The discrete frequencies have been chosen based on the sound transmission class with A-weighting constant. In order to prevent the softening effect occurrence due to optimization, stability analysis has been used as inequality constraint by ANSYS APDL. Several traditional composite materials have been taken for investigation. As a result, it has been found that an optimized composite plate made of stiffer materials (Graphite/Epoxy and Fiber carbon/RF) has better transmission loss characteristics in the stiffness region. However, in the mass control region, optimization of plies orientation has not effectively changed in the TL because of the close densities of composite materials. In addition to plies orientation, lamina thickness has a significant role in the TL. But it is necessary to ensure that the advantage of low-weight composite materials is not compromised by TL. The result has also demonstrated that, optimization of composite plate made of multimaterial has slightly different sound transmission characteristics.

References

- [1] Chandra N., Raja S., Gopal K.V., "Vibro-acoustic response and sound transmission loss analysis of functionally graded plates," *Journal of Sound and Vibration*, Vol. 333, pp.5786–5802, 2014.
- [2] Denli H., Sun J.Q., "Structural acoustic optimization of sandwich cylindrical shells for minimum interior sound transmission," *Journal of Sound and Vibration*, Vol. 316, pp.32–49, 2008.
- [3] Smith J. P., "Sound transmission through thin cylindrical shells," *Journal of Acoustical Society of America*, Vol. 29, pp.712–29, 1957.
- [4] White P., "Sound Transmission through a finite, closed, cylindrical Shell," *Journal of Acoustical Society of America*, Vol. 40, pp. 1124–30, 1966.
- [5] Koval L., R., "Sound Transmission into a Laminated Composite Cylindrical Shell," *Journal of Sound and Vibration*, Vol. 71, No.4, pp. 523-530, 1980.
- [6] Blaise A., Lesuer C., Gotteland M., Barbe M. "On sound transmission into an orthotropic infinite shell.comparison with Koval's results and understanding of phenomena," *Journal of sound and vibration*150: 233–43, 1991.
- [7] Lee J. H., Kim J., "Study on sound transmission characteristics of a cylindrical shell using analytical and experimental models," *Applied Acoustic*, Vol. 64, pp.611-632, 2003.
- [8] Roussos L.A., "Noise transmission loss of a rectangular plate in an infinite baffle," NASA Technical Paper 2398, 1985.
- [9] Lang M. A., Dym C. L., "Optimal acoustic design of sandwich panels," *Journal of the Acoustical Society of America*, Vol. 57, 1974, pp. 481-1487.
- [10] Wang T., Li S., Nutt S.R., "Optimal design of acoustical sandwich panels with a genetic algorithm," *Journal of Applied Acoustics*, Vol. 70, No. 3, pp. 416–425, 2009.
- [11] Tsai Y. T., Pawar S. J., Huang J., "Optimizing material properties of composite plates for sound transmission problem," *Journal of Sound and Vibration*, Vol.335, pp.174-186, 2015.
- [12] Nouri A., Astaraki, S., "Optimization of sound transmission loss through a thin functionally graded material cylindrical shell," *shock and vibration journal*, 2014, Article ID 814682.
- [13] Chakraborty A., Gopalakrishnan.S., "Wave propagation in inhomogeneous layered media: solution of forward and inverse problems," *Acta Mechanica*, Vol.169, 2004, pp. 53–185.
- [14] Geebelen N., Boeckx L., Vermeir G., Lauriks W., "A model for estimating the acoustic performances of multilayered systems based on a multiple extension of the transfer matrix method," *Proceedings of the Sixth European Conference on Noise Control, Finland*, pp.1–6, 2006.
- [15] R Talebitooti, A. M. Choudari Khameneh, M. R. Zarastvand, M. Kornokar, "Investigation of three-dimensional theory on sound transmission through compressed poroelastic sandwich cylindrical shell in various boundary configurations", *Journal of Sandwich Structure & Materials*, online.
- [16] Dijkmans A., Vermeir Glauriks., W., "Sound transmission through finite light weight multilayered structures with thin air layers," *Journal of Acoustical Society of America*, Vol.128, 2010, pp. 3513–3524.
- [17] R.Talebitooti, M.R.Zarastvand, "The effect of nature of porous material on diffuse field acoustic transmission of the sandwich aerospace composite doubly curved Shell", *Aerospace Science and Technology*, Volume 78, July 2018, Pages 157-170

- [18] R. Talebitooti, M. R. Zarastvand, H. D. Gohari, "Investigation of power transmission across laminated composite doubly curved shell in the presence of external flow considering shear deformation shallow shell theory", *Journal of Vibration and Control*, Vol. 24, Issue 19, 2018.
- [19] Crocker M. J., *Handbook of Acoustics*, John Wiley and Sons, New York, NY, USA, 1998.
- [20] Roy T., Chakraborty, D., "Optimal vibration control of smart fiber-reinforced composite shell structures using an improved genetic algorithm," *Journal of Sound and Vibration*, Vol. 319, 2009, pp. 15-40.
- [21] Bert C. W., "Optimal design of composite material plate to maximize its fundamental frequency," *Journal of sound and vibration*, Vol. 50, No. 2, 1977, pp. 229-237.
- [22] Jones R. M. (1999). *Mechanics of Composite Materials*, Taylor & Francis publication, second edition, USA.
- [23] David, A. B. and Hansen, C. H., *Engineering Noise Control Theory and Practice*, Spon Press, London, UK, fourth edition, 2009.
- [24] Fahy F. J. and Gardonio P., *Sound and Structural Vibration. Radiation, Transmission and Response*, Academic Press, San Diego, California, USA, second edition, 2007.
- [25] Conn A. R., Gould N. M. and Ph. L. Toint, "A Globally Convergent Augmented Lagrangian Barrier Algorithm for Optimization with General Inequality Constraints and Simple Bounds," *Mathematics of Computation*, Vol. 66, No. 217, 1997, pp. 261-288.
- [26] Standard practice for determining single-number rating of airborne sound isolation in multiunit building specifications, E597-81, Annual Book of ASTM Standards (American Society of Testing and Materials), Philadelphia, 1984.
- [27] Dym C. L., Lang, M. A., (1974), "Transmission of sound through sandwich panels", *Journal of the Acoustical Society of America*, Vol. 56, pp. 1523-1532, 1974.